Research Article **IJNR (2017) 1:2**

International Journal of Nanoparticle Research
(IJNR)

Solution Phase growth of Tin Oxide (SnO2) Nanostructures under Controlled Synthesis Conditions

M. A. Khan[1,2], Hasan Mahmood[*3,4], Bilal Mohuddin[1], Tariq Iqbal[1], Assad Qayyum[1], Ishaq Ahmed[5], Waleed Maqbool[1]

[1]Department of Physics, University of Azad Jammu and Kashmir, Muzaffarabad 13100, Pakistan; [2]High-Tech Lab., University of Azad Jammu and Kashmir, Muzaffarabad 13100, Pakistan; [3]Department of Physics, COMSATS Institute of Information Technology, Defense road Lahore, Pakistan; [4]Department of Physics, State University of New York at Albany, Albany, NY, 12222 USA; [5]National Center for Physics, Quaid-i-Azam University Campus Islamabad, Pakistan

ABSTRACT

Tin dioxide (SnO2) nanostructures have been synthesized successfully via solution phase growth technique. Effect of reaction temperature, time and surfactant on morphology, size and bandgap of nanomaterials has been studied. The rods, flowers and spheres like morphologies of SnO2 have been observed using Scanning Electron Microscope (SEM). Structural analysis of synthesized SnO2 has been carried out by X-ray Diffraction (XRD). XRD peaks revealed the tetragonal structure of SnO2 nanocrystals. The increase in grain size was observed with increase in reaction time and reaction temperature of synthesis process. Fourier Transform Infrared spectroscopy (FTIR) has been employed to study the vibrational modes. Optical properties of the SnO2 nanostructures have also been studied by UV-vis spectroscopy. The energy bandgap of the as prepared SnO2 nanocrystals was estimated between 3.76 eV and 4.05 eV. It has been observed that the bandgap of the synthesized SnO2 samples decreased with increase in particle size. This phenomenon can be attributed to the quantum confinement effect at smaller particle size.

Keywords: Crystalline SnO2; Nanorods and Nanoflowers; Bandgap; Quantum Confinement.

***Correspondence to Author:**
M. A. Khan
Department of Physics, University of Azad Jammu and Kashmir, Muzaffarabad 13100, Pakistan

How to cite this article:
M. A. Khan, Hasan Mahmood, Bilal Mohuddin, Tariq Iqbal, Assad Qayyum, Ishaq Ahmed, Waleed Maqbool. Solution Phase growth of Tin Oxide (SnO2) Nanostructures under Controlled Synthesis Conditions. International Journal of Nanoparticle Research, 2017; 1:2.

eSciencePublisher
eSciPub LLC, Houston, TX USA.
Website: http://escipub.com/

Introduction

Nanomaterials are important for researchers for advanced functional systems as well as wide-ranging applications because of their unique electronic, mechanical and optical properties. Nanomaterials behave differently from bulk materials due to certain factors i.e. shape, size etc. [1]. The bandgap of nanomaterials increases with decrease in particle size. The band in fact splits into discrete energy levels and so-called quantum sized effects occur. These quantum sized effects make nanomaterials valuable to use in optical devices. The growth of nanostructures with different morphologies such as nanoparticles, nanowires, nanorods etc. also have gained particular attention of materials research community. The great interest in the growth of nanostructures of different shapes is because of the fact that chemical and physical properties of nanomaterial highly depend upon aspect ratio and morphology [2, 3]. The properties of nanomaterials depend typically on the morphology, grain size and the specific surface area of the prepared nanomaterial.

The transition metal semiconducting oxides are an important class of semiconductors, which have large applications such as in magnetic storage media [4], solar energy transformation [5], gas sensors [6] and catalysis [7]. Among the most studied semiconducting oxides such as SnO_2, ZnO_2 and $InSnO_2$, SnO_2 is the most important because of its wide range of applications which is evident from large amount of papers reported in literature over the last decade [8]. SnO_2 is an n-type semiconductor with a wide direct bandgap of 3.62 eV [9]. The direct wide bandgap of SnO_2 makes it useful for optoelectronics devices. Nanostructured SnO_2 is also used as an active catalyst in many reactions [10, 11] and as electrodes of lithium-ion rechargeable batteries which have high capacity than conventional carbon based batteries [12].

SnO_2 also has many applications in electronics and optoelectronics. It is of great interest to use in surge arrestors (varistors) [13]. Two of the other most important reasons for the interest in this material are the high transparency in the visible region and high conductivity [8], which makes this material very useful for transparent conducting coatings for furnaces, electrodes [13], opto-conducting coatings for solar cells [14] and flat panel displays, etc. [8]. SnO_2 has also been widely used as a gas sensor due to the strong conductivity changes produced by chemi-absorbed gas molecules on its surface [15, 16]. Some aspects of SnO_2 depend strongly on the preparation methods too. As in nanoscale preparation, we observe the size quantization effects which have a lot of influence on the material properties [17]. There are numerous methods used for the synthesis of different nanomaterials. Among those, a solution based hydrothermal chemical route is a promising scheme for the synthesis of metal oxide nanostructures. Recently, the research on the shape control of various nanostructures has been developed because of their morphology dependent properties.

Extensive efforts have also been made by researchers to develop new methods ranging from template-assisted synthesis to conventional solution-phase routes to synthesize nanomaterials of desired dimensions and morphology [18]. SnO_2 nanocrystals have been synthesized by many technique like chemical vapor deposition [19], solvothermal route [20], carbothermal reduction [21], laser ablation technique [22] and calcination process [23] etc. All these techniques require a reaction temperature of 900 ^oC or higher which make it difficult for certain device applications and often control reproducibly is also difficult.

Here we present a simple method that requires low temperature for the synthesis of SnO_2 nanomaterials. Effect of reaction time, synthesis temperature and surfactant on the morphology, grain size and bandgap has been studied. The prepared nanostructures exhibited rod, flower and sphere like morphologies. The shape, nanoparticle size and their energy bandgap of the synthesized nanomaterials were found to be

controllable with temperature and reaction time of the experiment. The increase in particle size and decrease in bandgap have been observed with rise in temperature and reaction time.

Experimental

Synthesis

All the purchased chemicals were analytically pure. For the synthesis of SnO_2 nanocrystals, five precursor solutions were made beforehand: sample 01 was prepared by dissolving 1.05 g of $SnCl_4.5H_2O$ and 1.40 g of NaOH dissolved in a solution consisting of 40 ml of H_2O and 40 ml of ethanol. The precursor solution was then transferred to a stainless steel autoclave and heated at 180^o C for 24 h. The final precipitates were washed repeatedly with water and ethanol and then dried in vacuum at 60^o C for 16 h. The process can be shown schematically as in figure 1. Sample 02 was prepared at same reaction temperature with reaction time of 30 h. Sample 03 was prepared at reaction temperature of 200^o C with reaction time 24 h. Sample 04 was prepared by adding surfactant (Cetrimonium bromide or cetyltrimethylammonium bromide (CTAB)) keeping other reaction parameters same as that of sample 01. Sample 05 was prepared by increasing the reaction time 200^o C and keeping others parameters same as for sample 04. The parameters of all the prepared samples are summarized in the table 1 below;

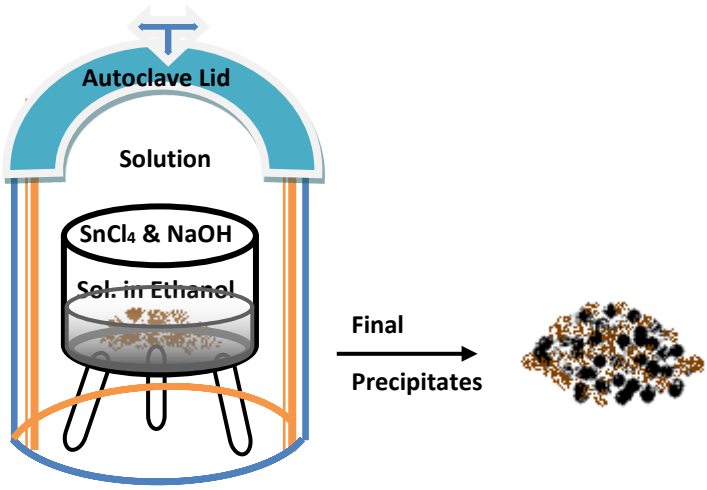

Figure 1: Schematics of Solution Phase growth technique

Table 1: Conditions for SnO_2 sample preparation

Sample No.	$SnCl_4.5H_2O$	NaOH	CTAB	Reaction Media	Reaction Time	Reaction Temperature
01	1.05 g	1.40 g	0 g	H_2O (40 ml) + ethanol (40 ml)	24 h	180^o C
02	1.05 g	1.40 g	0 g	H_2O (40 ml) + ethanol(40 ml)	30 h	180^o C
03	1.05 g	1.40 g	0 g	H_2O (40 ml) + ethanol(40 ml)	24 h	200^o C
04	1.05 g	1.40 g	2.18 g	H_2O (40 ml) + ethanol (40 ml)	24 h	180^o C
05	1.05 g	1.40 g	2.18 g	H_2O (40 ml) + ethanol (40 ml)	24 h	200^o C

Characterization

The prepared SnO_2 samples were subjected to various characterization techniques as X-Ray Diffraction (XRD), Scanning Electron Microscope (SEM), Fourier Transform Infrared (FTIR) spectroscopy and Ultraviolet-visible (UV-Vis) spectroscopy. The phase structure of these samples were studied by using Bruker AXS focus diffractometer with high intensity Cu K_α radiation (λ =0.1541 nm) in the 2θ range of 20-60^o. The morphology of the nanostructures was identified using Jeol JSM-6510 LV scanning electron microscope. For the calculation of bandgap, UV-visible absorption spectra were collected on Perkin-Elmer, LAMBDA 950 spectrometer by dissolving sample powders in ethanol. For vibrational analysis of bonds, Perkin-Elmer 100 Series FTIR spectrometer was used in the wave number range of 4000-400 cm^{-1}.

Results and Discussion

The structural analysis of as prepared SnO_2 was carried out by XRD. The XRD patterns of samples prepared under various reaction conditions are shown in figure 2. All the peaks are according to the JCPDS file No. 41-1445. XRD patterns of the samples confirmed highly crystalline phases of SnO_2 nanostructures. The obtained lattice constants a = 0.4742 nm and c = 0.3192 nm also pointed out that the nanocrystals belonged to tetragonal system.

To calculate particle size (D), the principal diffraction line (101) has been used in Scherrer formula.

$$D = \frac{C\lambda}{\beta \cos\theta}$$

Similar kind of behavior was shown by all other samples. Figure 1 also shows that with increase in reaction time and temperature, the width of peaks is decreasing which illustrates that with increase in reaction time and temperature, the particle size is increasing. The lattice constants were found to be same but the crystalline size was different. The crystalline sizes were found to be 17.12 nm, 26.51 nm, 28.25 nm, 23.80 nm, 32.14 nm and 29.5 nm for sample 01, sample 02, sample 03, sample 04 and sample 05 respectively. This shows that the reaction conditions have explicit effect on the particle size; there is an increase in particle size with increase in reaction temperature and time. Thus high temperature increases the vibrational energy of atoms for diffusive motion and thereby increasing the grain size [24]. The grain sizes of all 5 samples have been shown in table 2.

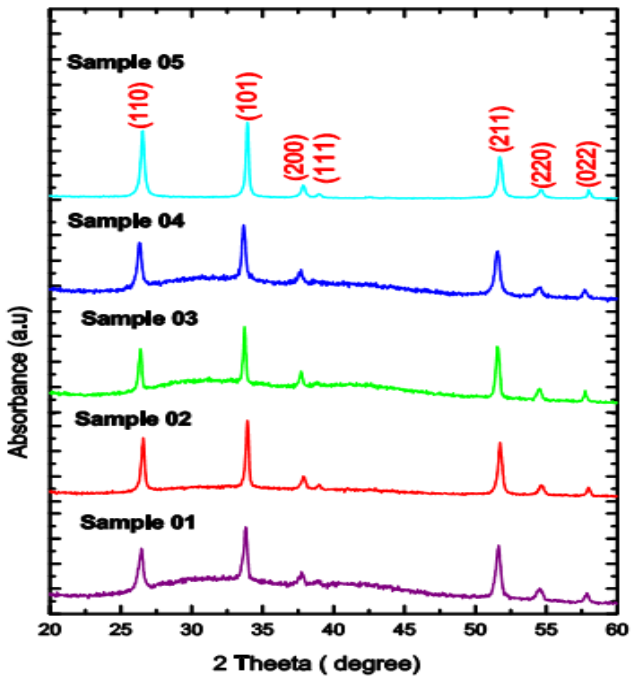

Figure 2: XRD patterns of all five Samples

The morphology identification of all five samples prepared under different reaction conditions was performed using SEM. Figure 3 shows the SEM images of sample 01, 02, 03, 04 and 05. Sample 01 shows rod like morphology. Sample 02 shows that with the increase in reaction time, the dimensions of rods are increased but morphology remains the same. Sample 03 shows that when reaction temperature is increased to 200^{o} C keeping reaction time 24 h the morphology is changed from nanorods to nanoflowers. Sample 04 shows with the addition of surfactant and keeping all other reaction parameters same as sample 01, the morphology is totally changed from nanorods to nanospheres. Sample 05 shows in the presence of surfactant when temperature is increased, the size of nanospheres are also increased. This showed that the morphology and size of nanomaterials were greatly affected by reaction parameters.

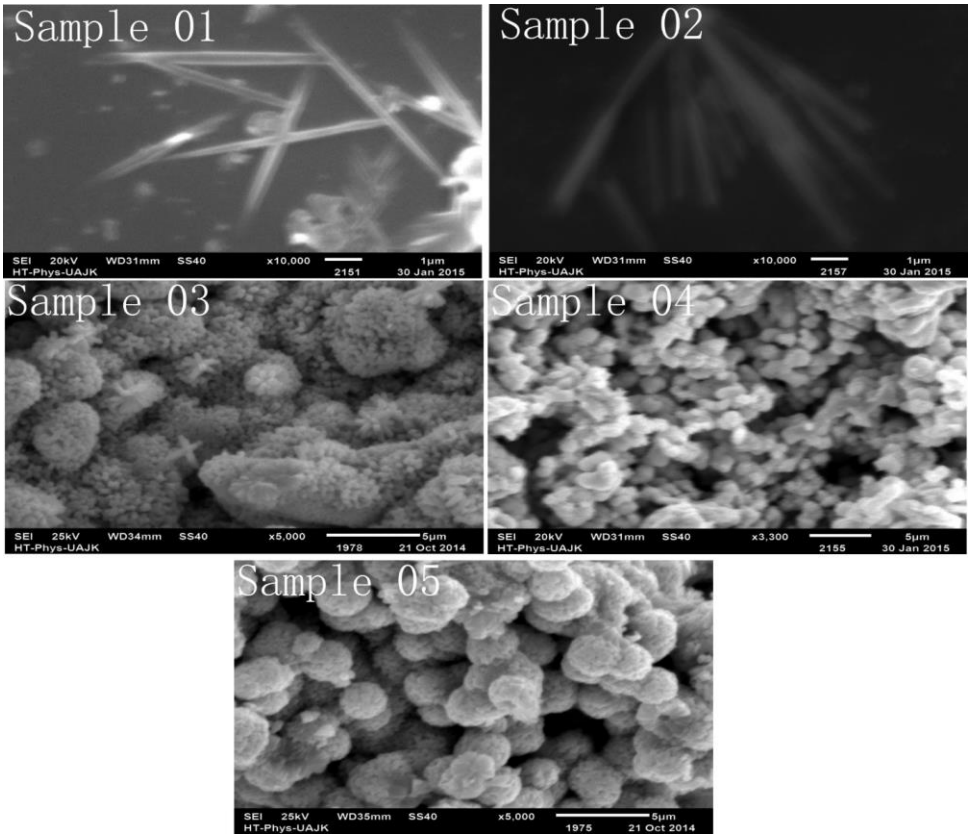

Figure 3: SEM images of SnO_2 nanostructures

Figure 4 represents the FTIR spectra of SnO_2 nanostructures. The peak around 650 cm^{-1} represents SnO_2 stretching vibrations [25]. The band 470 cm^{-1} can be attributed to bending vibrations of SnO_2. The bands around 1300 cm^{-1} are assigned to bending modes of Sn-OH. The symmetric stretching was also observed in the range 3400 $cm^{-1}$to 3700 cm^{-1} [26, 27]. The H-O-H bonding was observed around 1590 cm^{-1} [28]. Also here if we compare the spectra of sample 3 and sample 5, we see the maximum absorbance shifts towards shorter wavelength and this was because of the presence of surfactant CTAB in sample 5 while all other synthesis parameters were same in both samples 3 and 5.

The optical characterizations were carried out using Perkin-Elmer, LAMBDA 950 spectrometer in the wavelength range from 200 nm to 800 nm. In UV-vis absorption spectroscopy, the synthesized SnO_2 nanopowder was dissolved in absolute ethanol and subsequently SnO_2 nanoparticles were well dispersed in ethanol using ultrasonic vibration to form a true solution. The bandgap energies of all the samples were estimated using UV data. Figure 5 shows absorbance of all the samples. The peak

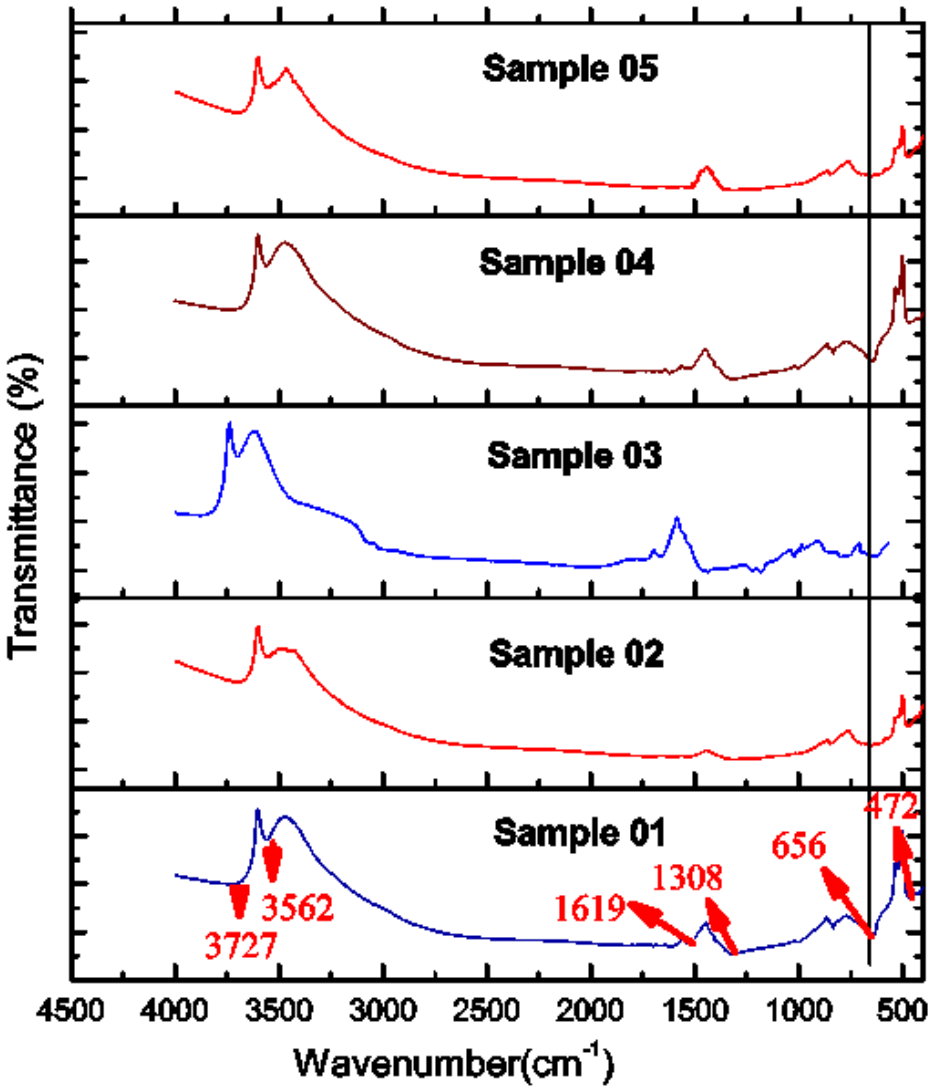

Figure 4: FTIR spectra of all prepared samples.

absorbance lies at wavelength 286 nm for sample 02, which indicates good absorption capability of SnO_2 for UV range.

We also see here, when the reaction temperature is increased keeping all other parameters same, the peak absorbance is shifted towards red i.e. 292 nm for sample 03. The peak shifting may be attributed to the change in the size of nanoparticles.

The bandgap energies of SnO_2 nanocrystal were estimated using the equation [29].

$$\alpha h\nu = K(h\nu - E_g)^n$$

Where α is the absorption coefficient, $h\nu$ is the incident photon energy, E_g is the bandgap energy, h is Planck constant, K is a proportionality constant. The value of n was chosen 1/2 because SnO_2 has direct energy bandgap. The bandgap energy E_g was calculated for all the samples by extrapolating the straight line of $(\alpha h\nu)^2$ vs. $h\nu$ plot to intercept on the horizontal energy axis as shown in figure 5.

The bandgap for sample 01 was found to be 4.05 eV. This value is greater than the 3.62 eV, which is bandgap for bulk SnO_2. This increase in bandgap at nano level is merely due to quantum effects [30]. The other values of bandgaps calculated from Tauc plots were 3.88 eV, 3.84 eV, 3.95 eV and 3.76 eV for sample 02, sample 03, sample 04 and sample 05, respectively as shown in figure 6. This result shows that the reaction temperature and reaction time have

significant effect on the bandgap of SnO_2 be attributed to the increase in the size of nanomaterials. The decrease in bandgap may nanoparticles.

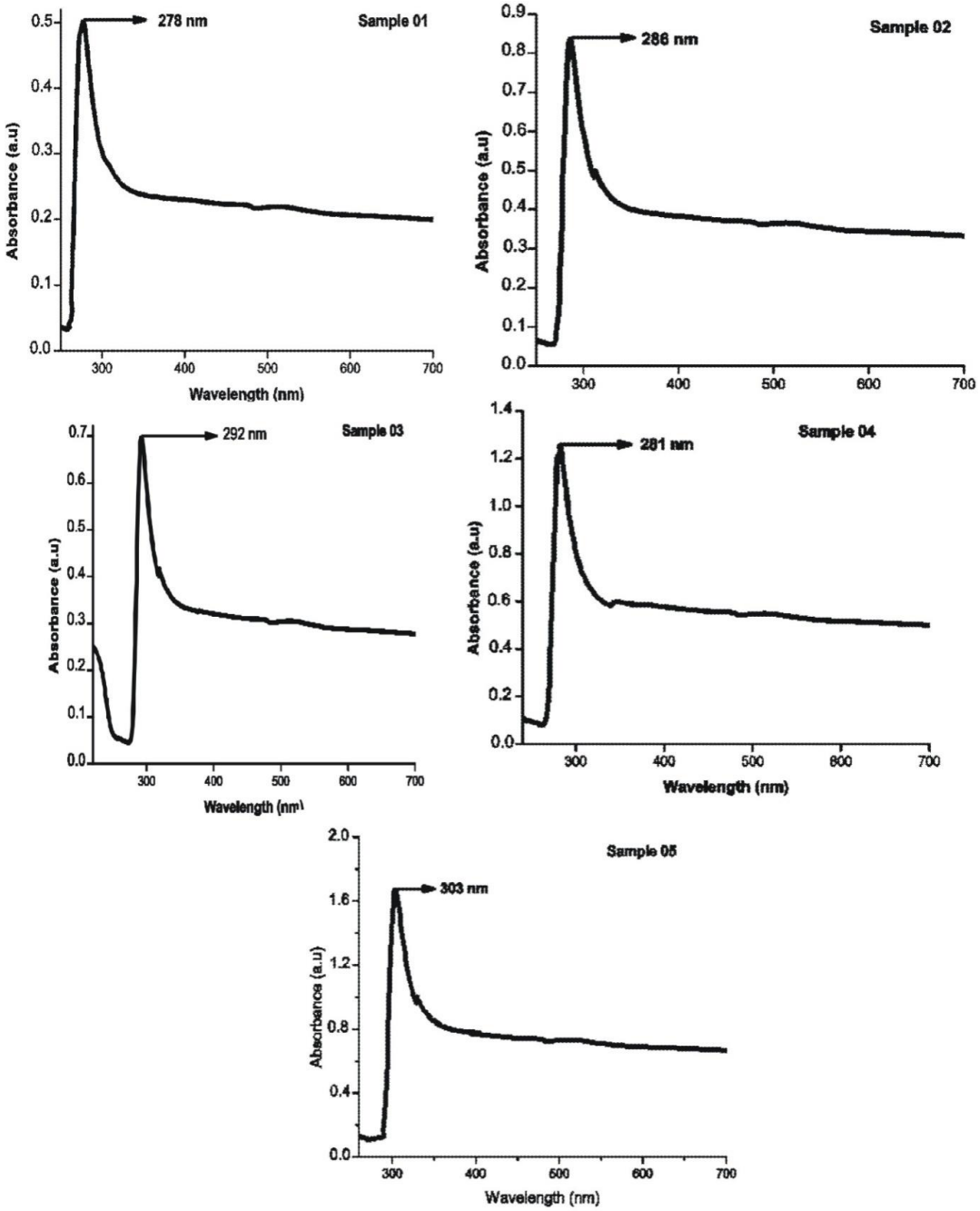

Figure 5: UV-Vis spectra of all SnO_2 nanostructure samples

Table 2: The summary of results under different conditions

Sample No.	Reaction Temperature	Reaction Time	Surfactant	Morphology	Grain Size	Bandgap
01	24 h	180° C	0 g	Nanorods	17.12 nm	4.05 eV
02	30 h	180°C	0 g	Nanorods	26.51 nm	3.88 eV
03	24 h	200°C	0 g	Nanoflowers	28.25 nm	3.84 eV
04	24 h	180°C	2.18 g	Nanospheres	23.80 nm	3.95 eV
05	24 h	200°C	2.18 g	Nanospheres	32.14 nm	3.76 eV

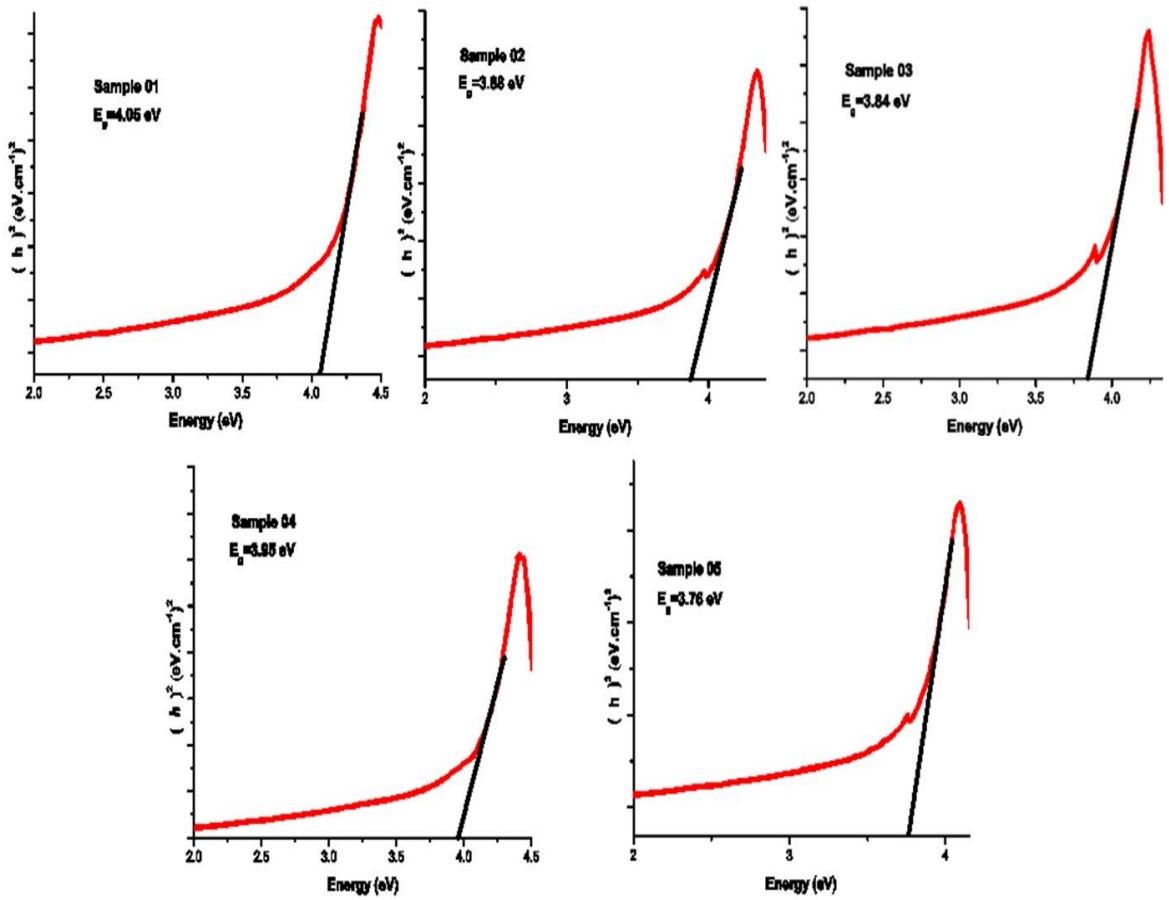

Figure 6: Tauc plot of SnO_2 nanostructures

Conclusions

Tin Oxide nanostructures i.e., nanorods, nanoflowers and nanospheres with different diameters and lengths have been synthesized through a simple solution phase growth technique. The effect of reaction parameters and surfactant on the morphology has been studied. It has been observed that reaction parameters and surfactant significantly affect the morphology of nanostructures. XRD pattern of as-prepared SnO_2 nanostructures showed crystalline form and rutile tetragonal phase of SnO_2. All the samples showed the same peaks at the values of 2θ that strongly indicates the formation of SnO_2 nanostructures. It has been observed that with increase in reaction time and temperature, the width of peaks decreases which confirms the increase in nanoparticle size. Therefore from above discussion it is concluded that reaction parameters greatly affect the nanocrystalline size. FTIR spectra also confirmed the presence of SnO_2 bands. UV-Vis absorption characteristics showed good absorbance capability in UV range. Optical bandgaps were also calculated using Tauc plot. It has been observed that with increase in reaction temperature or time bandgap decreases, which is due to increase in nanoparticle size. The synthesized SnO_2 nanostructures may have important application in fabrication of the solar cells and nano-devices.

References

[1] A. Hyo-Jin, C. Hyun-Chul, P. Kyung-Won, K. Seung-Bin, S. Yung-Eun, J. Phys. Chem. B. 2004;108:9815-9820

[2] Z.W. Pan, Z. R. Dai, Z. L. Wang, Science. 2001;291:1947

[3] A. P. Alivisatos, Science. 1996;271:933

[4] K. Nagase, Y. Zheng, Y. Kodama and J. Kakuta, Journal of Catalysis. 1999;187:123-130

[5] M. Yin, C. K. Wu, Y. Lou, C. Burda, J. T. Koberstein and Y. Zhu, Journal of American Chemical Society. 2005;127:9506-9511

[6] V. Zhang, J. Liu, Q. Peng, X. Wang and Y. Li, Chemistry of Materials. 2006;18:867-871

[7] H. Wu, D. Lin and W. Pan, Applied Physics Letters. 2006;89:1-3
[8] L. L. D. Flores, R. R. Bon, A. M. Galvan, E. Prokhorov and J. G. Hernandez, Journal of Physics and Chemistry of Solids. 2003;64:1037–1042
[9] O. Lupana, L. Chowa, G. Chaic, A. Schultea, S. Parka and H. Heinricha, Materials Science and Engineering B. 2009;157:101–104
[10] A. I. Ahmed, S.A. El-Hakam, A.S. Khder and W.S. Abo El-Yazeed, Journal of Molecular Catalysis A: Chemical. 2013;366:99–108
[11] N. S. Fallah and M. Mokhtary, Journal of Taibah University for Science. 2015;9:531–537
[12] Y. Idota, T. Kubota, A. Matsufuji, Y. Maekawa and T. Miyasaka, Science. 1997;276:1395
[13] S. A. Pianaro, P. R. Bueno, E. Longo, J.A. Varela, J. Mater. Sci. Lett. 1995;14:692
[14] K. L. Chopra, S. Major, D. K. Pandya, Thin Solid Films. 1983;102:1
[15] R. Rella, A. Serra, P. Siciliano, L. Vasanelli, G. De, A.Licciulli, A. Quirini, Sensors Actuators B. 1997;44:462
[16] R. Rella, P. Siciliano, S. Capone, M. Epifani, L. Vasanelli, A.Licciulli, Sensors Actuators B. 1999;58:283
[17] M. A. Khan, H. Mahmood, R. N. Ahmed, A. A. Khan, Mahboobullah, Tariq Iqbal, A. Ishaque and R. Mofeed, Journal of Nano Research. 2016;40:1-7
[18] O. Lupan, L. Chow, G. Chai, B. Roldan, A. Naitabdi, A. Schulte, Mater. Sci. Eng. B. 2007;145:57
[19] D. Calestani, M. Zha, A. Zappettini, L. Lazzarini, G. Salviati, L. Zanotti, G. Sberveglieri, Mater. Sci. Eng. C. 2005;25:625
[20] G. Cheng, K.Wu, P. Zhao, Y. Cheng, X. He, K. Huang, J. Cryst. Growth. 2007;309:53
[21] J. X. Wang, D. F. Liu, X. Q. Yan, H. J. Yuan, L. J. Ci, Z. P. Zhou, Y. Gao, L. Song, L. F. Liu, W. Y. Zhou, G. Wang, S. S. Xie, Solid State Commun. 2004;130:89
[22] Z. Q. Liu, D. H. Zhang, S. Han, C. Li, T. Tang, W. Jin, X. L. Liu, B. Lei, C. W. Zhou, Adv. Mater. 2003;15:1754
[23] M. Li, Q. Lu, Y. Nuli, X. Qian, Electrochem. Solid-State Lett. 2007;10:33–37
[24] W. D. Callister, D. G. Rethwisch, Fundamentals of Materials Science and Engineering, John Wiley & Sons, 3rd edition, 2007
[25] L. Tan, L. Wang and Y. Wang. Jour. Nanoma. 2011;7:1-10
[26] S.Y. Venyaminov and F. G. Prendergast; Anal. Biochem. 1997;248:234-245
[27] D. N. Srivastava, S. Chappel, O. Palchik, A. Zaban and A. Gedanken. 2002;18:4160-4164
[28] M. Jean Standard, Chemistry, Introduction to Molecular Vibrations and Infrared Spectroscopy; 2013
[29] S. Tsunekawa, T. Fukuda, A. Kasuya; Journal of Applied Physics. 2000;87:1318-1321
[30] R. S. Rossetti, S. Nakahara and L. E. Brus; J. chem. phys. 1983;79:1086